

Automated reconstruction of soil stress-strain response from full field displacement measurements and loading data using optimisation

Reconstruction automatisée de la réponse contrainte-déformation du sol à partir de mesures de déplacement sur le terrain complet et de données de chargement en utilisant l'optimisation

J. A. Charles

University of Sheffield, Sheffield, United Kingdom

C. C. Smith, J. A. Black

University of Sheffield, Sheffield, United Kingdom

ABSTRACT: The significant amounts of image data that can be generated during physical model tests can provide a useful alternative and direct route to determining the stress-strain response characteristics of the soil used in the model without recourse to e.g. sampling and triaxial testing. Using optimisation, it is possible to find the stress-strain curve such that internal work calculated using the Particle Image Velocimetry (PIV) derived full-field displacement data is equal to external work. Whereas previously published work by the authors optimized for the unknown stress-strain curve by splitting it piecewise into many hundreds of segments, an alternate formulation presented in this work instead allows the description of the curve based on constitutive models, with only a handful of optimization variables necessary. FEA derived “perfect” data sets are reused to validate the new formulation. The eventual goal of the methodology is the robust application of the method to physical modelling test data, this paper presents a milestone towards this goal.

RÉSUMÉ: Les quantités importantes de données d'image pouvant être générées au cours des tests sur modèles physiques peuvent constituer une alternative utile et une voie directe pour déterminer les caractéristiques de réponse contrainte-déformation du sol utilisé dans le modèle sans avoir recours, par exemple, à l'échantillonnage et essais triaxiaux. En utilisant l'optimisation, il est possible de trouver la courbe de contrainte-déformation de sorte que le travail interne calculé à l'aide des données de déplacement sur champ complet dérivées de la vélocimétrie image par particule (PIV) soit égal au travail externe. Alors que les travaux précédemment publiés des auteurs optimisaient la courbe contrainte-déformation inconnue en la découpant par morceaux en plusieurs centaines de segments, une formulation alternative présentée dans ce travail permet plutôt de décrire la courbe sur la base de modèles constitutifs, avec seulement une poignée d'optimisation variables nécessaires. Les ensembles de données «parfaits» dérivés de la FEA sont réutilisés pour valider la nouvelle formulation. L'objectif final de la méthodologie est l'application robuste de la méthode aux données d'essais de modélisation physique. Le présent document présente une étape importante dans la réalisation de cet objectif.

Keywords: Back analysis; Identification method; Soil response; PIV; Optimization;

1 INTRODUCTION

Numerical modelling of soils presents the significant challenge of precisely determining the stress-strain response of the soil, typically in terms a chosen constitutive model with associated parameters.

The ability to accurately measure said parameters through element tests such as triaxial tests or in-situ tests such as cone penetrometer tests involves overcoming issues such as sample representativeness or disturbance.

The current work leverages advances in Particle Image Velocimetry (PIV) within geotechnical engineering (White et al. 2001) to utilize the full field displacement data of a sample undergoing testing as a means of recovering unknown parameters.

PIV is non-invasive and provides no disturbance to a sample undergoing testing. Imaging equipment and a transparent sample box are the only requirements, along with textured soil such that the movement of soil patches can be tracked over time using Digital Image Correlation. For soils without texture, such as kaolin clay, floc can be applied.

An Identification Method is a procedure by which unknown properties of a material can be recovered based on measured loading data and PIV (or another imaging process) derived displacement data. The field of material science has developed numerous variations on this method, typically applied to small metallic samples, which have been catalogued and described at length by Avril et al. (2008). Although there are significant variations between methods, the primary goal is to find optimal material properties such that a modelled response of a sample is as close to its physically measured response as possible.

The goal of this work is to apply these methods to geotechnical engineering. Numerous challenges relating to the realities of soil will be necessary to overcome, such as complex stress-strain responses, non-uniform deformations, imaging issues, and potential out of plane effects.

Initial work by Gueguin et al. (2015) demonstrated a proof of concept method applying a simplified version of the Virtual Field Method (VFM), as developed by Grédiac & Pierron (1998), to geotechnical problems. Past contributions by the authors of this paper built on this work by demonstrating the validity of the method for preliminary physical model tests (Charles et al. 2018b) and investigating the effects of noise application to complex artificially derived FEA datasets (Charles et al. 2018a).

This contribution approaches the problem from a different angle. Whereas the aforementioned work by the authors describes the stress-strain response as a curve with an arbitrary number of segments, each with an individually optimized stiffness, this contribution describes the stress-strain response with an equation with just a few parameters. Although arbitrary equations could be used to describe the curve (i.e. a quadratic equation with 3 unknowns), typical geotechnical equations are both more relevant and likely to provide a better fit to the data. This work focusses on a linear-elastic perfectly-plastic response, and a nonlinear elastic plastic power law response.

After a derivation of the Identification Method, a demonstration of validity using FEA derived idealised data will be presented, and ongoing work towards validation by physical modelling will be discussed.

2 IDENTIFICATION METHOD FORMULATION

2.1 Principles of the Identification Method

The identification method functions based on the principle of conservation of energy. External work applied to a soil sample (e.g. by loading or due to gravity) must be equal to the internally dissipated work. However, as shown in Charles et al. (2018a), physical realities of measurement disallow an exact match. As such, for a system with

strain field ε , and stress field σ , the following equation must be satisfied for each timestep j :

$$W_{int}^{(j)}(\sigma, \varepsilon) + EnergyGap^{(j)} = W_{ext}^{(j)} \quad (1)$$

Where $W_{int}^{(j)}$ represents internal work expended during timestep j , and is a function of the stress and strain fields, and $W_{ext}^{(j)}$ represents external work between said timesteps, and is the work done by the applied loading. The purpose of this method is to find the stress field such that the absolute energy gap throughout all timesteps is minimised:

$$Minimize \sqrt{\sum_{j=1}^J timesteps (EnergyGap^{(j)})^2} \quad (2)$$

Although more complex loading cases are possible, in this contribution external work will consist of a known point load displacing by a known amount. As such, External work $W_{ext}^{(j)}$ is the area under the force-displacement curve for time step j , with $F(u)$ being the force corresponding to displacement u and can be shown with the following equation:

$$W_{ext}^{(j)} = \int_{u^{j-1}}^{u^j} F du \quad (3)$$

As stated by Charles et al. (2018a), internal work $W_{int}^{(j)}$ is a function of the stress and strain fields integrated across the whole field area A , which can be discretised into E elements, and can be shown with the following equation:

$$W_{int}^{(j)} = \sum_{e=1}^E \left(\int_{\varepsilon_s^{j-1,e}}^{\varepsilon_s^{j,e}} 2t d\varepsilon_s \right) \quad (4)$$

Where t is deviatoric stress, and ε_s is shear strain, which are calculated from the eigenvalues of the stress field (σ_1, σ_2) and strain field ($\varepsilon_1, \varepsilon_2$). The equation essentially finds the area under the stress-strain curve for each element, and sums them for each time step.

Note that this is a simplification based on the assumption of zero volumetric strain and associative flow. Although these assumptions are valid for the plane strain tests on uniform undrained clay, additional terms could be added to allow for different soil behaviours.

2.2 Constitutive parameter based optimization

In order to calculate the internal work expended during a timestep, the area under the stress-strain curve for each element must be found. The change in shear strain is known as it can be calculated from the PIV derived displacement field. The corresponding stress values however are unknown. They must thus be found such that the energy gap is optimally small.

In the previously cited work by the authors of this contribution, the stress-strain curve was split into an arbitrary number of segments, each of which would be provided a stress value as an output of the optimization process, requiring potentially hundreds of variables to obtain a realistic curve.

In this contribution however, the soil response will be assumed to follow a specified constitutive model, and as such, only the much smaller number of constitutive parameters would be needed to be optimized in order to adequately describe the curve.

In order to formulate the problem into a form that can be optimized for, it is necessary to define $W_{int}^{(j)}$ for each time step in terms of the unknown constitutive parameters. For the trivial case of a rigid perfectly plastic response, the unknown constitutive parameter peak shear stress τ_{max} , can be multiplied by the change in shear strain to find the area under the curve. This area can be calculated independently and summed for each of E elements, with subscript e referring to element number. Thus, for a 3 timestep problem, internal work can be found with the following matrix multiplication:

$$\begin{pmatrix} W_{int}^{(1)} \\ W_{int}^{(2)} \\ W_{int}^{(3)} \end{pmatrix} = \begin{pmatrix} \sum_{e=1}^E 2\delta\varepsilon_s^{1,e} \\ \sum_{e=1}^E 2\delta\varepsilon_s^{2,e} \\ \sum_{e=1}^E 2\delta\varepsilon_s^{3,e} \end{pmatrix} (\tau_{max}) \quad (5)$$

This is similarly trivial for a linear elastic response with Young's modulus as the only variable, as area under the stress strain curve can easily be expressed in terms of an unknown gradient. A linear elastic perfectly plastic response can be found by combining the aforementioned responses. Internal work would be taken as the areas under the two separate parts of the response simply added together. The elastic limit would become a third variable.

More complex multi-variable models such as the nonlinear elastic power law equation (Vardanega & Bolton 2011), shown in Equation 6, provide more challenge.

$$\tau = \frac{c_u}{2} \varepsilon_s^b \varepsilon_{sm2}^{-b} \quad (6)$$

τ represents the shear stress at shear strain ε_s along the stress-strain curve. c_u is the peak shear stress, ε_{sm2} is the shear strain at which half the peak stress is achieved, and b is a dimensionless variable. The internal work is the area under the curve, which can be obtained through integration. The following equation shows the internal work for a timestep j with a single element:

$$W_{int}^{(j)} = \int \frac{c_u}{2} \varepsilon_s^b \varepsilon_{sm2}^{-b} \delta\gamma = \frac{c_u}{2(b+1)} \varepsilon_{sm2}^{-b} (\varepsilon_{sj}^{b+1} - \varepsilon_{sj-1}^{b+1}) \quad (7)$$

This equation has some significant challenges to overcome to adapt for optimization. Several unknowns are exponents, or multiplied together, making linear optimization impossible. Fortunately, b is limited to a small range of values (0.3 to 0.9) such that multiple attempts with varying pre-set b can be run, and c_u can be estimated prior to optimization by finding the optimal rigid plastic, or linear elastic rigid plastic response. Finally, with known b , ε_{sm2}^{-b} can be taken as the variable

to be optimized, giving the internal work matrix for an example 3 timestep problem as:

$$\begin{pmatrix} W_{int}^{(1)} \\ W_{int}^{(2)} \\ W_{int}^{(3)} \end{pmatrix} = \begin{pmatrix} \sum_{e=1}^E \frac{c_u}{2(b+1)} (\varepsilon_{s1,e}^{b+1} - \varepsilon_{s0,e}^{b+1}) \\ \sum_{e=1}^E \frac{c_u}{2(b+1)} (\varepsilon_{s2,e}^{b+1} - \varepsilon_{s1,e}^{b+1}) \\ \sum_{e=1}^E \frac{c_u}{2(b+1)} (\varepsilon_{s3,e}^{b+1} - \varepsilon_{s2,e}^{b+1}) \end{pmatrix} (\varepsilon_{sm2}^{-b}) \quad (8)$$

Note the subscripts refer to the timestep number, for example $\varepsilon_{s2,e}^{b+1} - \varepsilon_{s1,e}^{b+1}$ refers to the shear strain in timestep 1, element e , subtracted from the shear strain in timestep 2, element e .

In this work, a combined approach will be presented. Firstly, the optimal linear-elastic rigid plastic response for each test will be reconstructed. Secondly, the nonlinear elastic plastic power law response will be reconstructed, assuming the c_u value based on the peak stress observed during the linear elastic rigid plastic curve, with a range of b values attempted. Furthermore, due to the simplicity of the constitutive models used, the parameters can be found using a brute force approach instead of optimization. Although crude and inefficient, this will allow for contour plots showing clearly how adjusting variables effects the energy gap.

3 DEMONSTRATION OF METHOD USING FEA SIMULATED DATA

3.1 Methodology

During the development of new methodologies, it is useful to remove as many complicating factors as possible. Physical modelling has issues such as noise, discretization, out of plane effects, and experimental error that although necessary to deal with in the future, can be avoided by substituting FEA generated displacement data for real PIV data.

Measures have been taken to ensure that the FEA generated data is representative of real soil such that it can be treated as “perfect” data for the purposes of development, testing and validating the identification method. The fine details of the FEA models used to generate validation data sets are given in Charles et al. (2018a), but an abridged and adapted specification is detailed in the following paragraphs. Abaqus CAE (Dassault Systems 2017) was used to generate the datasets.

The model consists of a 2d, 8m by 8m, block of soil undergoing deformation due to a rotating wall with a point load at the edge furthest to the hinge. Although any loading case should work, the rotating wall was chosen due to having no singularities within the FEA modelled response. Figure 1 illustrates the set up. 512 uniform 6 node triangular elements were used, and the soil was modelled as weightless and isotropic. Nodal displacements were used in place of PIV patch displacements as inputs to the identification method.

The soil response was modelled as clay undergoing strain hardening. The stress-strain response input into the FEA software was generated using the nonlinear elastic plastic power law equation, with a perfectly plastic plateau. Values used to generate the curve were $b = 0.5$, $\gamma_{m2} = 0.05$, and $c_u = 100kPa$. The input curve will be shown in comparisons in the following section.

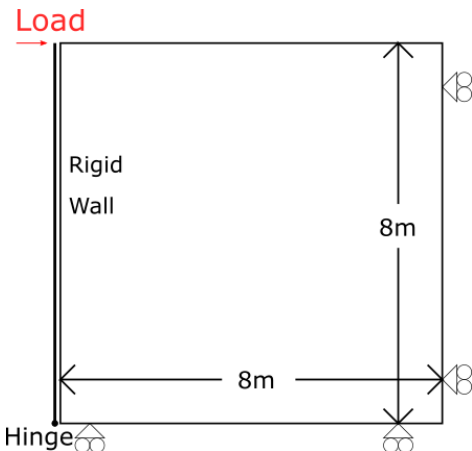


Figure 1: A representation of the FEA model used to generate validation datasets. Taken from Charles et al. (2018a).

The FEA model was run with 10 timesteps of length 0.5 seconds. Loading applied to the rotating wall increased linearly from 0MN to 1MN throughout the test. A plot of the strain field, showing maximum shear strain ϵ_s , (referred to as “max in-plane principle” in the Abaqus plot), is shown in Figure 2.

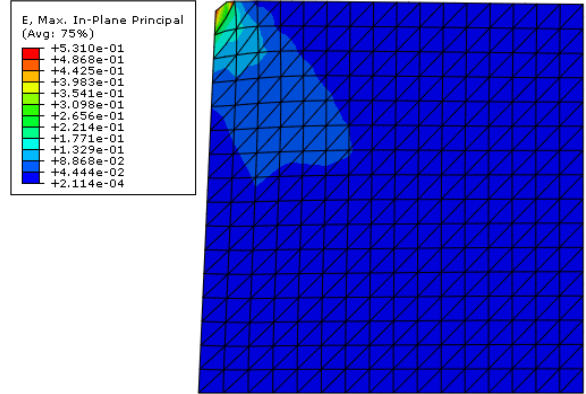


Figure 2: A plot of the strain field produced by the FEA simulation

3.2 Results and Discussion

As stated in Section 2.2, the constitutive parameters will be recovered through a two stage process, first recovering the linear elastic rigid plastic response, and using this as the starting point for the reconstruction of a nonlinear power law response.

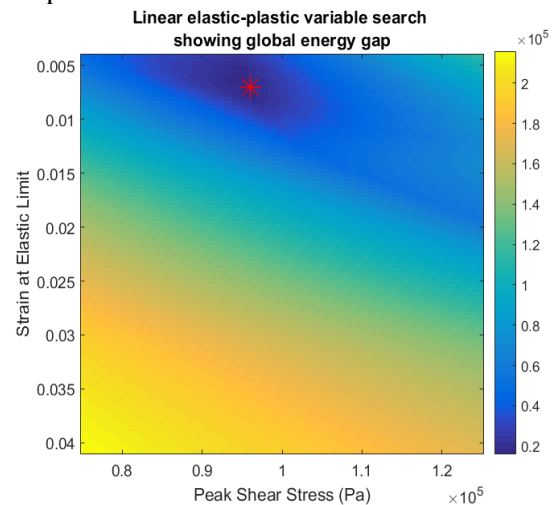


Figure 3: Variable contour plot for linear curve

The first step reconstructed a curve with a high energy gap (around 5.5%). This high energy gap was expected as it was an attempt to fit a response to data that is known not to match, with the intention of estimating c_u . Figure 3 shows the variable search area and figure 4 shows the curve comparison.

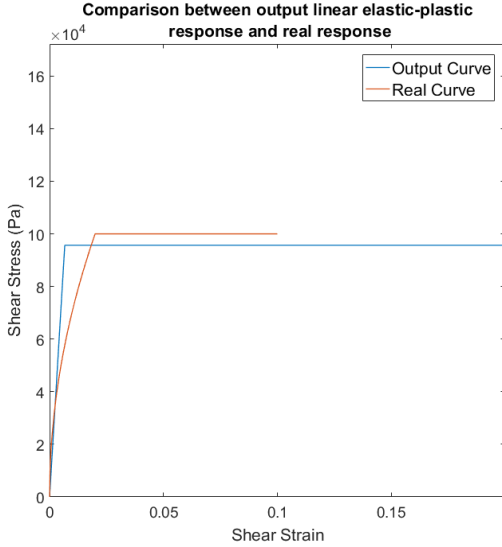


Figure 4: Comparison between output and expected responses for linear case

The second step involved using the peak shear stress c_u from the linear elastic rigid plastic curve as a known value for recovering the nonlinear power curve law response. Although it would be possible to use c_u as a third variable in a 3 dimensional search, significant time is saved by using an initial estimate which can then be varied slightly. An initial c_u of 96kPa was taken based on the results of the linear elastic rigid plastic response, this was varied up and down by up to 5% in order to find the true global best parameter set. Figures 5 and 6 show the variable search areas for the original and final c_u values respectively and Figure 7 shows a comparison between the reconstructed curve and input curve. An energy gap of about 1.3% was found using the presumed c_u value, reducing to 0.24% when allowing it to vary. The final constitutive parameters obtained are shown in the following graph:

Table 1. Comparison between expected and obtained parameters

Parameter	Expected	Output Value
b	0.5	0.507
ϵ_{sm2}	0.05	0.042
c_u	100kPa	98.5kPa

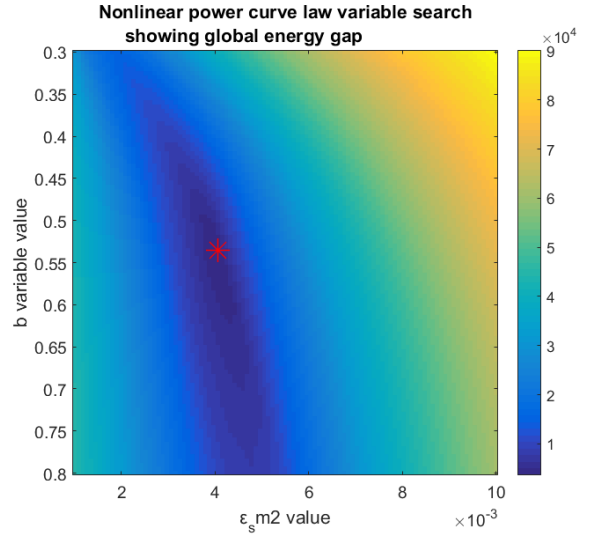


Figure 5: Variable contour plot for nonlinear curve for presumed c_u of 96kPa

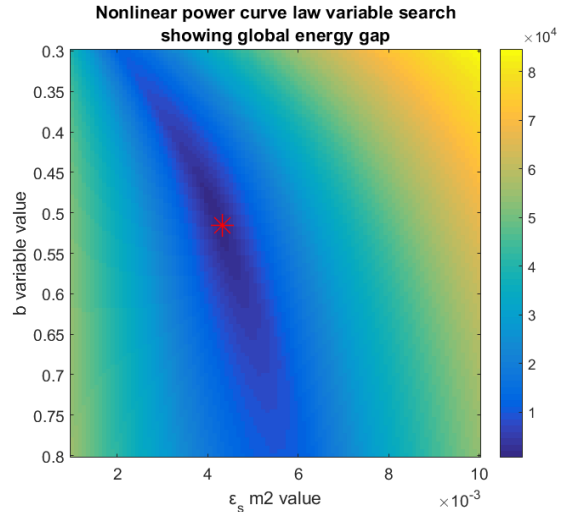


Figure 6: Variable contour plot for nonlinear curve for improved c_u of 98.5kPa

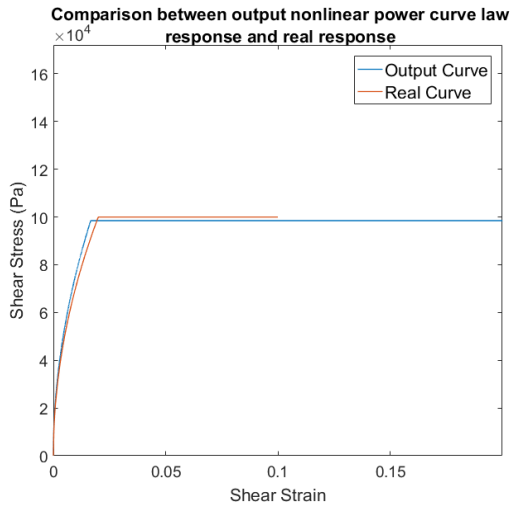


Figure 7: Comparison between output and expected responses for nonlinear case. See Table 1 for comparison of parameters

Although the reconstructed response is very close to the actual response there is still a slight difference. Constitutive parameters obtained were reasonable, with a slightly conservative c_u value obtained. The contour plots add confidence that the method is able to obtain the true best response, as opposed to one of many potentially valid output curves with negligible energy differences.

The differences between the reconstructed output curve and the real curve are possibly due to discretization within the FEA model, or trace amounts of volumetric strain (Abaqus limits poissons ratio to 0.49999, as opposed to 0.5). Work is ongoing to develop and further refine the procedure.

4 ONGOING WORK TO DEMONSTRATE OF METHOD USING PHYSICAL MODELLING DATA

A round of physical model tests is currently underway and will be presented at ECSMGE 2019. The purpose of these tests is to obtain high quality datasets with which the identification method

procedure can be validated and improved. A summary of the testing is as follows:

Footing tests are to be carried out on undrained Kaolin clay samples, mixed and consolidated from powder to 200kPa, 300kPa, and 400kPa, with loading applied via a 20mm or 40mm aluminium footing using a strain based actuator moving at ~ 0.1 mm/s. The velocity of the actuator was chosen such that the assumption of undrained behaviour, and thus, zero volumetric strain was valid. Force-settlement data will be recorded with a load cell and LVDT. A photograph of the experimental setup used in preliminary testing can be seen in figure 8.

Image data will be collected using industrial Ethernet cameras at a rate of 2.5fps. GeoPIV-RG (Stanier et al. 2015) will be used to calculate the full field displacement data.

Footing tests have been chosen due to simplicity of testing. The method should be valid for any possible loading scenario.



Figure 8: The rig used for preliminary testing

5 CONCLUSIONS

An adaption to the previously presented geotechnical Identification Method has been demonstrated that allows the recovery of arbitrary constitutive parameters. Current work demonstrates the method functions adequately using perfect artificial data for undrained clays with nonlinear stress-strain responses. The choice of artificial data sets should not affect the method; however, this contribution is limited to showing a single scenario due to space limitations.

Progress towards demonstration with real physical modelling data has been reported, along with issues identified with preliminary data sets.

Future work will primarily consist of generation of high quality data sets through physical modelling. Additionally, the software framework developed to facilitate the constitutive parameter based identification method, should allow for reconstructing curves based on arbitrary models for undrained clay. Additions of capability for other soil types, e.g. frictional or those undergoing volumetric strain could potentially be implemented.

6 ACKNOWLEDGEMENTS

The primary author acknowledges the PhD Studentship provided by the UK Engineering and Physical Sciences Research Council (EPSRC).

7 REFERENCES

- Avril, S., M. Bonnet, A. S. Bretelle, M. Grédiac, F. Hild, P. Ienny, F. Latourte, D. Lemosse, S. Pagano, E. Pagnacco, & F. Pierron (2008). Overview of identification methods of mechanical parameters based on full-field measurements. *Experimental Mechanics* 48(4), 381–402.
- Charles, J.A, Smith, C. C, Black, J, A (2018a). Evaluating the effects of noise on full field displacement data used for the identification of soil stress-strain response. *Numerical Methods in Geotechnical Engineering IX. NUMGE 2018*. 221-226.
- Charles, J.A, Smith, C. C, Black, J, A (2018b). Identification of soil stress-strain response from full field displacement measurements in plane strain model tests. *Physical Modelling in Geotechnics. ICPMG 2018*. 835-840.
- Dassault Systems (2017). Abaqus cae finite element analysis software. <https://www.3ds.com/products-services/simulia/products/abaqus/abaqus-cae/>.
- Grédiac, M. & F. Pierron (1998). A T-shaped specimen for the direct characterization of orthotropic materials. *International Journal for Numerical Methods in Engineering* 41(September 1996), 293–309.
- Gueguin, M., C. Smith, & M. Gilbert (2015). Use of digital image correlation to directly derive soil stress-strain response from physical model test data, pp. 3881–3886.
- Stanier, S. A., J. Blaber, W. A. Take, & D. J. White (2015). Improved image-based deformation measurement for geotechnical applications. *Canadian Geotechnical Journal* 13 (October 2015), 1–35.
- Vardanega, P. J., & Bolton, M. D. (2011). Strength mobilization in clays and silts. *Canadian Geotechnical Journal*, 48, 1485–1503.
- White, D. J., W. A. Take, & M. Bolton (2001) Measuring soil deformation in geotechnical models using digital images and PIV analysis. *10th International Conference on Computer Methods and Advances in Geomechanics*, 997–1002.